

**NANO EXPRESS**

**Open Access**

# Graphitic carbon grown on fluorides by molecular beam epitaxy

Sahng-Kyoon Jerng, Jae Hong Lee, Yong Seung Kim and Seung-Hyun Chun<sup>\*</sup>

## Abstract

We study the growth mechanism of carbon molecules supplied by molecular beam epitaxy on fluoride substrates ( $MgF_2$ ,  $CaF_2$ , and  $BaF_2$ ). All the carbon layers form graphitic carbon with different crystallinities depending on the cation. Especially, the growth on  $MgF_2$  results in the formation of nanocrystalline graphite (NCG). Such dependence on the cation is a new observation and calls for further systematic studies with other series of substrates. At the same growth temperature, the NCG on  $MgF_2$  has larger clusters than those on oxides. This is contrary to the general expectation because the bond strength of the carbon-fluorine bond is larger than that of the carbon-oxygen bond. Our results show that the growth of graphitic carbon does not simply depend on the chemical bonding between the carbon and the anion in the substrate.

**Keywords:** Graphene, Graphitic carbon, Molecular beam epitaxy, Fluoride

**PACS:** 81.05.uf, 81.15.Hi, 78.30.Ly

## Background

From the success of graphene growth on Ni or Cu by chemical vapor deposition (CVD) [1,2], some variations were introduced to CVD to avoid the use of metallic catalysts [3-8]. However, the growth of carbon by chemical methods involves a complex mechanism due to the presence of carrier gases. For example, hydrogen acts as an etching reagent as well as a co-catalyst [9]. In contrast, physical deposition methods such as molecular beam epitaxy (MBE) are useful to understand the growth mechanism of carbon because of the relatively simple kinetics [10-13]. Experimentally, it has been shown that nanocrystalline graphite (NCG) could be formed on crystalline and amorphous oxides by direct sublimation of carbon [14-16]. Although first-principles calculations partly explained that the strong bonding between carbon and oxygen limited the cluster size [14,16], the growth mechanism is yet to be understood.

So far, carbon MBE has been tried on substrates containing elements from group IV [10-13], group V [17], and group VI [12,14-16]. Here, we present the results of carbon MBE on fluorides (where the anion belongs to group VII) and compare them with similar studies on

oxides to understand the effect of the anion on the quality of NCG. Since the bonding between carbon and fluorine is much stronger than the bonding between carbon and oxygen, we expected the carbon film to be more amorphous. On the contrary, NCG of good crystallinity was formed on  $MgF_2$ , and the cluster size deduced from Raman spectra was even larger than those of NCGs on  $MgO$  and sapphire [18,19]. These results show that the quality of NCG does not simply depend on the bond strength of carbon and substrate anion, and imply that the carbon growth mechanism could be more complex than previously thought.

## Methods

### Materials and film fabrication

Carbon MBE was done using a home-made ultra-high-vacuum MBE system and a carbon sublimation cell with a pyrolytic graphite filament. The pressure of the chamber was kept below  $1.0 \times 10^{-7}$  Torr during the growth by flowing liquid nitrogen in the shroud. Details about the growth procedure can be found elsewhere [14]. Fluoride substrates ( $MgF_2(100)$ ,  $CaF_2(100)$ , and  $BaF_2(111)$ ) were purchased from a commercial vendor (CrysTec GmbH, Berlin, Germany). The growth temperature was fixed at 900°C because of the lower melting points of fluoride substrates compared to oxides.

\* Correspondence: schun@sejong.ac.kr

Department of Physics and Graphene Research Institute, Sejong University, Seoul 143-747, South Korea

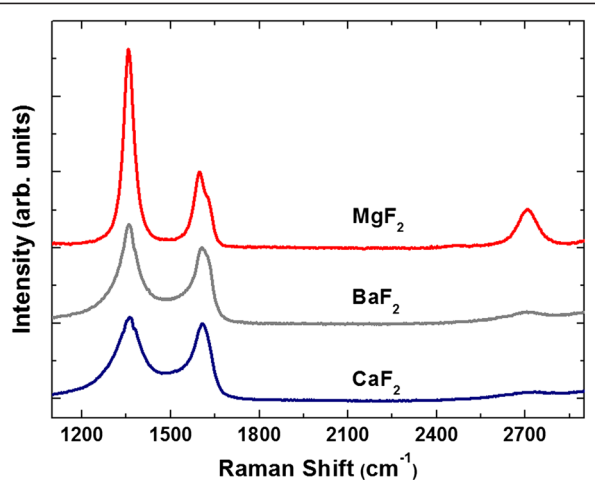


**Figure 1** Raman spectra of carbon films. The films were grown by carbon MBE at 900°C on  $\text{MgF}_2(100)$ ,  $\text{CaF}_2(100)$ , and  $\text{BaF}_2(111)$ . The pronounced 2D peak at approximately 2,700  $\text{cm}^{-1}$  confirms that nanocrystalline graphite is formed on  $\text{MgF}_2$ .

### Characterization

Raman scattering measurements and spatial mapping were performed using a micro-Raman spectrometer (inVia system, Renishaw, Wotton-under-Edge, UK) operated by a 514.5-nm laser. A minimal laser power of 2 mW was used during the measurements to avoid any damage or heating of the carbon films. Atomic force microscopy (AFM) images were taken by a commercial system (NanoFocus Inc., Seoul, South Korea) in a non-contact mode. AFM in a contact mode was also used to determine the film thickness by measuring the step height after lithography. X-ray photoelectron spectroscopy (XPS) measurements to analyze carbon bonding characteristics were done using a

**Table 1** Fitting results of the Raman spectra from the graphitic carbon on  $\text{MgF}_2$

|                               | D     | G     | 2D    |
|-------------------------------|-------|-------|-------|
| Position ( $\text{cm}^{-1}$ ) | 1,348 | 1,601 | 2,685 |
| FWHM ( $\text{cm}^{-1}$ )     | 44    | 61    | 83    |
| $I/I_G$                       | 2.8   | 1     | 0.5   |

Lorentzian functions are used to fit D, G, and 2D peaks. FWHM, full width at half maximum.

Kratos X-ray photoelectron spectrometer (Kratos Analytical Ltd, Manchester, UK) with Mg K $\alpha$  X-ray source. C1s spectra were acquired at 150-W X-ray power with a pass energy of 20 eV and a resolution step of 0.1 eV.

### Results and discussion

Figure 1 shows the Raman spectra from 3- to approximately 5-nm-thick carbon films grown on various fluorides by MBE. The characteristic peaks of graphitic carbon are well identified in all films: the D peak at approximately 1,350  $\text{cm}^{-1}$  and the G peak at approximately 1,590  $\text{cm}^{-1}$ . These and previous studies show that MBE is an effective method for graphitic carbon growth on a wide range of substrates [14-17]. The degree of graphitization is, however, quite different depending on the cation. In fact, graphitic carbon refers to a wide range of disordered graphite, from NCG to mainly  $sp^2$  amorphous carbon. As clarified by Ferrari [20], the relative strength of D and G peaks alone cannot determine the degree of disorder, and it is the 2D peak at approximately 2,700  $\text{cm}^{-1}$  which distinguishes NCG from amorphous carbon. As shown in Figure 1, the Raman spectra of the carbon film on  $\text{MgF}_2$  show a clear 2D peak, indicating that successful NCG growth

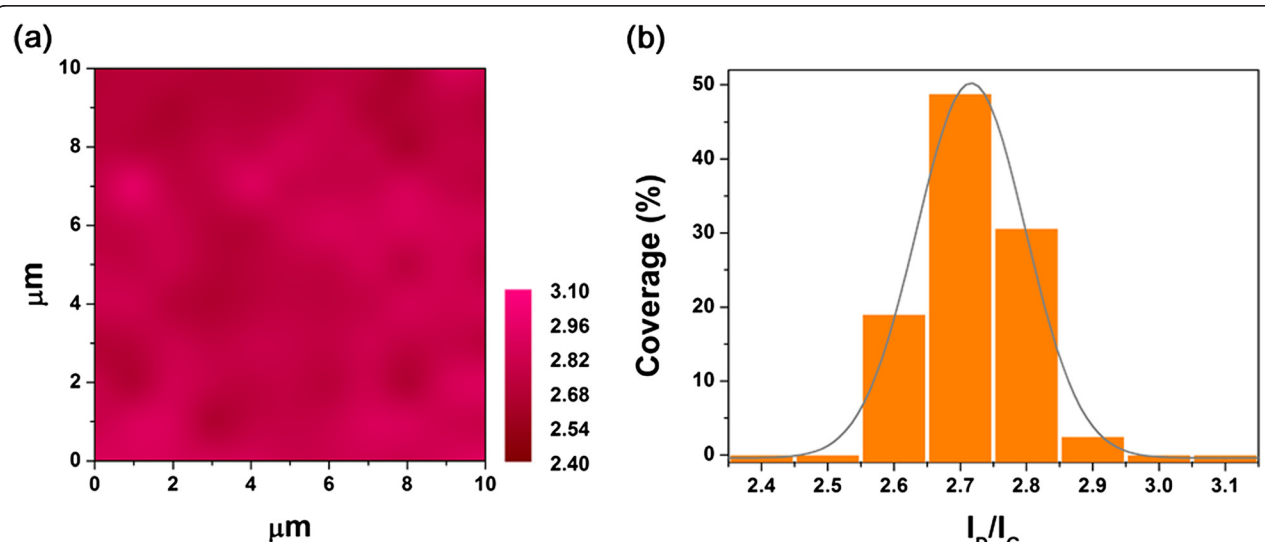


**Figure 2** Raman map of graphitic carbon on  $\text{MgF}_2$ . (a) The intensity ratio of the D peak to the G peak is mapped over 10  $\times$  10  $\mu\text{m}$ . The distributions, shown in (b), imply a high spatial uniformity.

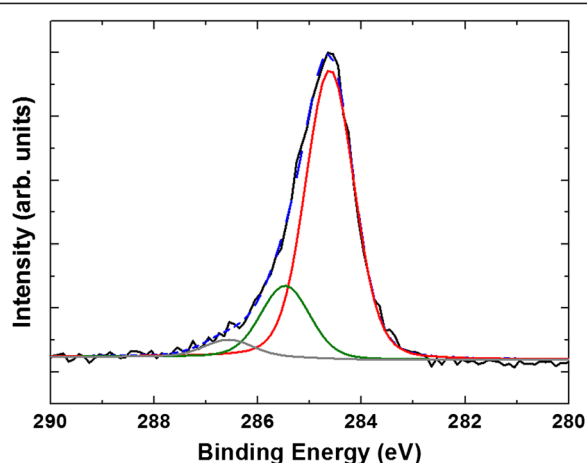


**Figure 3** C1s XPS spectra of graphitic carbon on  $\text{MgF}_2$ . The dashed line is a fit with four Lorentzian functions. The two strongest peaks (centered at 284.6 eV (red) and 285.8 eV (green)) are assigned to  $sp^2$  and  $sp^3$  hybridized carbon atoms, respectively. The fraction of the  $sp^2$  bond is estimated to be 80.1%.

was accomplished on  $\text{MgF}_2$  by carbon MBE. In contrast, the carbon films grown on  $\text{CaF}_2$  and  $\text{BaF}_2$  can be ascribed to amorphous carbon. As far as we know, carbon MBE on a family of substrates having the same anion has not been reported. Clear understanding of this cation dependence is yet to come, but our results will stimulate systematic studies on other series of substrates and further theoretical investigations.

We will focus on the growth on  $\text{MgF}_2$  from now on and compare the results with NCGs on oxides. For a quantitative comparison, the Raman spectra of NCG on  $\text{MgF}_2$  were fit by several Lorentzian functions as in [15] (Table 1). Interestingly, the intensity ratios of the D peak and 2D peak to the G peak ( $I_D/I_G$  and  $I_{2D}/I_G$ ) are larger than those from NCG on  $\text{MgO}$ . Furthermore, all the peaks are narrower, implying a better crystallinity on  $\text{MgF}_2$  (from the comparisons of the full width at half

maximum (FWHM) in Table 1 and those in [15]). The average cluster size,  $L_a$ , can be calculated from the relation  $I_D/I_G = C L_a^2$ , where  $C = 0.0055$  and  $L_a$  in Å [20]. From  $I_D/I_G = 2.7$  (Table 1), we get  $L_a = 22 \text{ \AA}$ , a slight increase from those on oxides [15,16]. Figure 2 shows a Raman map of the intensity ratio of  $I_D/I_G$  over  $10 \mu\text{m}^2$ . Most regions have  $I_D/I_G = 2.7 \pm 0.1$ , thus showing a high degree of uniformity. The uniformity is also better than that of NCG on  $\text{MgO}$  [16].

All these results indicate that NCG on  $\text{MgF}_2$  is less disordered than those on oxides. This is quite surprising if we consider the bond strength of the C-F bond, which is larger than the C-O bond strength [18,19]. The high electronegativity of fluorine even makes the C-F bond partially ionic. From first-principles calculations, we have known that the strong C-O bond limits the cluster size of NCG on sapphire and  $\text{MgO}$  [14,16]. If that is the whole story, the stronger C-F bond should lead to smaller clusters on  $\text{MgF}_2$ . Our results against this imply that an important factor is missing in the theoretical understanding of the NCG growth mechanism. Recently, models such as the catalytic role of step edges or the migration of cyclic carbons are good examples of pertinent suggestions [4,21].

Figure 3 presents XPS results to clarify the carbon bonding characteristics. Similar to previous studies [14,16],  $284.7 \pm 0.2$  and  $285.6 \pm 0.2$  eV components in C1s spectra are attributed to  $sp^2$  and  $sp^3$  bonds [22], namely,  $sp^2$  hybridization of carbon atoms and  $sp^3$  hybridization of C-C or C-H bonds, respectively [23]. The fitting results show that the fraction of the  $sp^2$  bond is more than 80%, confirming the NCG formation on  $\text{MgF}_2$ .

Finally, Figure 4 shows AFM images before and after the NCG growth on  $\text{MgF}_2$ . Unlike crystalline and amorphous oxide substrates, the mean roughness parameter,  $R_a$ , of the  $\text{MgF}_2$  substrate is large. The  $R_a$  of NCG (2.45 nm over  $1 \times 1 \mu\text{m}$  scan) is even larger by an

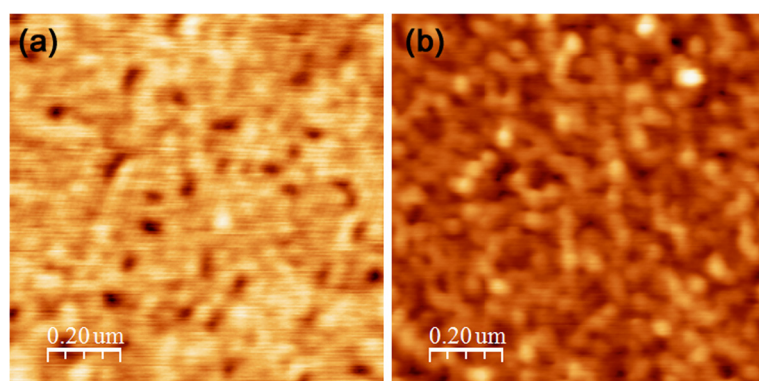


**Figure 4** AFM images of graphitic carbon on  $\text{MgF}_2$ . AFM images of  $1 \times 1 \mu\text{m}$  (a) before and (b) after the graphitic carbon growth on  $\text{MgF}_2$ . The mean roughness parameters,  $R_a$ , from  $1 \times 1 \mu\text{m}$  scans are (a) 0.97 and (b) 2.45 nm, respectively.

order of magnitude than those NCGs on oxide substrates [14–16]. It is not clear why the surface morphology is worse while the Raman spectra indicate a better crystallinity. We hope that the understanding of NCG growth on MgF<sub>2</sub> can lead to better NCG or possibly graphene growth on other (flat) dielectrics.

## Conclusions

In summary, we have grown graphitic carbon on fluoride substrates, expanding the application of carbon MBE into group VII anions. While amorphous carbons were formed on CaF<sub>2</sub> and BaF<sub>2</sub>, nanocrystalline graphite of good crystallinity was formed on MgF<sub>2</sub> despite the strong bonding between carbon and fluorine. In comparison to similar studies on MgO, the effect of the substrate anion on the quality of NCG contradicts the expectation based on the bond strength between carbon and the anion. Further systematic studies and theoretical investigations are encouraged to understand the carbon growth mechanism by MBE.

## Abbreviations

AFM: Atomic force microscopy; CVD: Chemical vapor deposition; FWHM: The full width at half maximum; MBE: Molecular beam epitaxy; NCG: Nanocrystalline graphite; XPS: X-ray photoelectron spectroscopy.

## Competing interests

The authors declare that they have no competing interests.

## Authors' contributions

SKJ carried out the carbon molecular beam epitaxy experiments and X-ray photoelectron spectroscopy. JHL carried out the atomic force microscopy measurements. YSK characterized the thin films by Raman spectroscopy. SHC designed the experiments and wrote the manuscript. All authors read and approved the final manuscript.

## Acknowledgments

This research was supported by the Priority Research Centers Program (2012-0005859), the Basic Science Research Program (2012-0007298, 2012-040278), the Center for Topological Matter in POSTECH (2012-0009194), and the Nanomaterial Technology Development Program (2012M3A7B4049888) through the National Research Foundation of Korea (NRF) funded by the Ministry of Education, Science and Technology (MEST).

Received: 6 December 2012 Accepted: 27 December 2012

Published: 3 January 2013

## References

1. Kim KS, Zhao Y, Jang H, Lee SY, Kim JM, Kim KS, Ahn J-H, Kim P, Choi J-Y, Hong BH: Large-scale pattern growth of graphene films for stretchable transparent electrodes. *Nature* 2009, **457**:706–710.
2. Li X, Cai W, An J, Kim S, Nah J, Yang D, Piner R, Velamakanni A, Jung I, Tutuc E, Banerjee SK, Colombo L, Ruoff RS: Large-area synthesis of high-quality and uniform graphene films on copper foils. *Science* 2009, **324**:1312–1314.
3. Su CY, Lu AY, Wu CY, Li YT, Liu KK, Zhang W, Lin SY, Juang ZY, Zhong YL, Chen FR, Li LJ: Direct formation of wafer scale graphene thin layers on insulating substrates by chemical vapor deposition. *Nano Lett* 2011, **11**:3612–3616.
4. Scott A, Dianat A, Bormert F, Bachmatiuk A, Zhang SS, Warner JH, Borowiak-Palen E, Knupfer M, Buchner B, Cuniberti G, Rummeli MH: The catalytic potential of high-kappa dielectrics for graphene formation. *Appl Phys Lett* 2011, **98**:073110.
5. Kidambi PR, Bayer BC, Weatherup RS, Ochs R, Ducati C, Szabó DV, Hofmann S: Hafnia nanoparticles – a model system for graphene growth on a dielectric. *Phys Status Solidi Rapid Res Lett* 2011, **5**:341–343.
6. Song HJ, Son M, Park C, Lim H, Levendorf MP, Tsen AW, Park J, Choi HC: Large scale metal-free synthesis of graphene on sapphire and transfer-free device fabrication. *Nanoscale* 2012, **4**:3050–3054.
7. Bi H, Sun SR, Huang FQ, Xie XM, Jiang MH: Direct growth of few-layer graphene films on SiO<sub>2</sub> substrates and their photovoltaic applications. *J Mater Chem* 2012, **22**:411–416.
8. Medina H, Lin YC, Jin CH, Lu CC, Yeh CH, Huang KP, Suenaga K, Robertson J, Chiu PW: Metal-free growth of nanographene on silicon oxides for transparent conducting applications. *Adv Funct Mater* 2012, **22**:2123–2128.
9. Vlassiouk I, Regmi M, Fulvio PF, Dai S, Datskos P, Eres G, Smirnov S: Role of hydrogen in chemical vapor deposition growth of large single-crystal graphene. *ACS Nano* 2011, **5**:6069–6076.
10. Hackley J, Ali D, DiPasquale J, Demaree JD, Richardson CJK: Graphitic carbon growth on Si(111) using solid source molecular beam epitaxy. *Appl Phys Lett* 2009, **95**:133114.
11. Al-Temimi A, Riedl C, Starke U: Low temperature growth of epitaxial graphene on SiC induced by carbon evaporation. *Appl Phys Lett* 2009, **95**:231907–231907-3.
12. Maeda F, Hibino H: Thin graphitic structure formation on various substrates by gas-source molecular beam epitaxy using cracked ethanol. *Jpn J Appl Phys* 2010, **49**:04DH13–04DH13-6.
13. Moreau E, Godey S, Ferrer FJ, Vignaud D, Wallart X, Avila J, Asensio MC, Bourrel F, Gallet JJ: Graphene growth by molecular beam epitaxy on the carbon-face of SiC. *Appl Phys Lett* 2010, **97**:241907.
14. Jerng SK, Yu DS, Kim YS, Ryou J, Hong S, Kim C, Yoon S, Efetov DK, Kim P, Chun SH: Nanocrystalline graphite growth on sapphire by carbon molecular beam epitaxy. *J Phys Chem C* 2011, **115**:4491–4494.
15. Jerng SK, Yu DS, Lee JH, Kim C, Yoon S, Chun SH: Graphitic carbon growth on crystalline and amorphous oxide substrates using molecular beam epitaxy. *Nanoscale Res Lett* 2011, **6**:565.
16. Jerng SK, Lee JH, Yu DS, Kim YS, Ryou J, Hong S, Kim C, Yoon S, Chun SH: Graphitic carbon growth on MgO(100) by molecular beam epitaxy. *J Phys Chem C* 2012, **116**:7380–7385.
17. Jerng SK, Yu DS, Lee JH, Kim YS, Kim C, Yoon S, Chun SH: Carbon molecular beam epitaxy on various semiconductor substrates. *Mater Res Bull* 2012, **47**:2772–2775.
18. O'Hagan D: Understanding organofluorine chemistry. An introduction to the C-F bond. *Chem Soc Rev* 2008, **37**:308–319.
19. Lemal DM: Perspective on fluorocarbon chemistry. *J Org Chem* 2004, **69**:1–11.
20. Ferrari AC: Raman spectroscopy of graphene and graphite: disorder, electron–phonon coupling, doping and nonadiabatic effects. *Solid State Comm* 2007, **143**:47–57.
21. Lippert G, Dabrowski J, Yamamoto Y, Herziger F, Maultzsch J, Lemme MC, Mehr W, Lupina G: Molecular beam growth of micrometer-size graphene on mica. *Carbon* 2013, **52**:40–48.
22. Ermolieff A, Chabli A, Pierre F, Rolland G, Rouchon D, Vannuffel C, Vergnaud C, Baylet J, Semeria MN: XPS, Raman spectroscopy, X-ray diffraction, specular X-ray reflectivity, transmission electron microscopy and elastic recoil detection analysis of emissive carbon film characterization. *Surf Interface Anal* 2001, **31**:185–190.
23. Luo Z, Yu T, Kim K-j, Ni Z, You Y, Lim S, Shen Z, Wang S, Lin J: Thickness-dependent reversible hydrogenation of graphene layers. *ACS Nano* 2009, **3**:1781–1788.

doi:10.1186/1556-276X-8-11

Cite this article as: Jerng et al.: Graphitic carbon grown on fluorides by molecular beam epitaxy. *Nanoscale Research Letters* 2013 **8**:11.